energies

MDPI

Article

Sensor Technology Options for Municipal Solid Waste Characterization for Optimal Operation of Waste-to-Energy Plants

Harald Ian D. I. Muri *,† and **Dag Roar Hjelme** †

Department of Electronic Systems, Norwegian University of Science and Technology, 7491 Trondheim, Norway; dag.hjelme@ntnu.no

* Correspondence: harald.muri@ntnu.no

† These authors contributed equally to this work.

Abstract: Reuse, refurbishing, and recycling are the most sustainable options for handling waste materials. However, for municipal solid waste (MSW) that is highly heterogenic, crude, contaminated, and decrepit, thermal conversion in waste-to-energy (WtE) plants is an option. In such plants, the fuel quality of MSW is difficult to predict and the substantial changes expected are challenging for incineration stability. Development of new online sensor technologies for monitoring waste properties prior to incineration is therefore needed. Sensors may contribute to increase WtE process stability, as well as reducing the probability of incineration stops or emissions exceeding legal limits. In this work, the operating principles of potential sensor systems for waste monitoring are categorized and assessed to be implemented for providing parameters for process control or indicators for process alarms in the waste incineration process. For transmissive settings, the use of inductance and hard X-ray sensors are most promising, whereas for reflective settings, utilization of photonic, inductive, soft and hard X-ray, as well as low-frequency radiowave sensors, are most promising. The analytic capacity of single-point measurements with inductance, radiowave, photonic, or X-ray sensors are limited to providing indicators for process alarms, whereas spectral imaging with X-ray or photonic techniques are feasible for providing parameters for both process control and indicators for process alarms. The results obtained in this sensor assessment will be important as a first step in guiding the evolution of monitoring waste properties in the WtE industry to increase repeatability, performance of energy production, and manual labor safety in controlling the waste incineration.

Keywords: waste-to-energy; waste characterization; sensor technologies; online monitoring; feasibility studies

Citation: Muri, H.I.D.I.; Hjelme, D.R. Sensor Technology Options for Municipal Solid Waste Characterization for Optimal Operation of Waste-to-Energy Plants. *Energies* **2022**, *15*, 1105. https://doi.org/10.3390/en15031105

Academic Editor: Idiano D'Adamo

Received: 6 December 2021
Accepted: 30 January 2022
Published: 2 February 2022

1. Introduction

Municipal solid waste (MSW) that is highly heterogenic, crude, contaminated, and decrepit cannot be handled for reuse, refurbishing, or recycling. Such MSW materials are usually landfilled or incinerated at waste-to-energy (WtE) plants. In view of a sustainable future, landfills should only be used for pretreated waste. Thus, for waste streams for which material recovery is not applicable, energy recovery using WtE plants is the path to follow [1–3]. Due to variation in feedstock properties, WtE plants are today operated with significant process safety margins, resulting in limited energy efficiency. Thus, to increase the competitiveness of the WtE sector, optimization of the incineration process is needed. To this effect, significant efforts have been turned towards sensors that could provide supplementary information regarding the physical and chemical properties of the fuel before it enters the combustion process. Information from such sensors, if integrated with the process control system, could be used to automatically adjust the process to increase stability of the energy production and avoid emissions exceeding legal limits or excessive

fouling and corrosion. As a minimum, the process must be adapted to the strong variations in the specific heat content and humidity of the waste.

While the use of sensor technologies to monitor and control the incineration process is well-established in all WtE plants, no plants utilize sensors to provide information regarding the properties of the waste fed into the incinerator; rather, various strategies for bunker management and waste mixing are implemented to improve the process control performance. However, these strategies have limitations due the handling of the large and bulky waste volumes on the WtE facility resulting in low mixing frequency. On the other hand, sensor technologies are routinely used for waste handling in plants for automated sorting and recovery of recyclable materials. Recently, several reviews have addressed this approach [4–8]. Unfortunately, the results from these studies are not transferable to the challenge we address in this paper. First of all, a waste sorting plant entails a completely different organization of waste handling compared with a conventional WtE plant. The waste handling process strongly impacts what kind of sensor technologies are applicable as well as how the sensor systems are implemented. Whereas in a waste sorting plant the sensors may interact with smaller quantities of waste in a serial manner, the waste handling in a WtE plant requires monitoring in bulk quantities. Second, the type as well as the quality of information required is very different in a waste sorting plant and a WtE plant. The process controller in a WtE plant needs both process-relevant parameters in addition to a process alarm parameter (e.g., to warn about potential dangerous waste compositions). Therefore, studies of sensor technologies for online monitoring of waste entering the incineration process must start with a new look at both the applicable sensor technologies as well as the applicable sensor system configurations. We are not aware of any published studies addressing the sensor needs and possibilities for this application. We note that Hitachi have started to address this need, as described in a recent paper [9].

Our objective with this first paper is to give the first input to this evolving need in the WtE industry. The main contribution is the comprehensive sensor technology assessment, including sensor technologies as diverse as sensors based on low-frequency electronic sensors, such as resistive and capacitive sensors, to sensors based on high-energy particles propagation in waste materials. The working principles of such sensors are very different from one sensor system to another. The great variety of sensor solutions available that could provide parameters for determining relevant properties, or fuel quality, of the WtE feedstock are exemplified from previous work in [4,10–13]. Thus, identification of the most appropriate sensor systems for fuel quality monitoring in WtE plants requires pairing the various working principles with implementation constraints and abilities for specific monitoring applications. The understanding of working principles will impose limitations and elucidate the usability of the sensor technologies for waste characterization. With holistic properties of the available waste monitoring systems established, it is possible to detail the sensor techniques further to provide feedforward parameters for the WtE process, such as for process control or for process alarm indicators. A first step in achieving waste classification on general waste properties prior to incineration on a WtE plant has been shown in [14].

The sensor assessment and feasibility studies in this paper are organized as follows. The waste fuel properties, possible problematic waste, and its impact on the incineration process are presented in Section 2. The literature review on the principles of the waste sensor systems, considering the interaction of the generated sensor input with matter, as well as the physical variables and constants affecting the detected signal output are presented in Section 3. In Section 4, the methods used for the feasibility assessment and assumption in moisture measurement computations are described. Next, in Section 5, the monitoring feasibility is assessed based on the sensor principles presented in Section 3. Finally, the findings on sensor implementation for transmissive or reflective settings for process control or alarms are summarized in Section 6.

2. Waste Properties and Impact on Incineration

2.1. Heating Value, Combustion Rate, and Problematic Materials

The combination of different waste materials contains desired or undesired features as fuel. The fuel quality of waste encompasses features such as total energy content, combustibility, and to which degree that it does not cause problems for the waste-to-energy process. In this section, the fuel quality is described in terms of the heating value, combustion rate, and problematic content of waste. This is further used for the assessment of sensor technology options in Section 3.

2.1.1. Heating Value

MSW as combustible materials are generally characterized experimentally by bomb calorimeter or predicted by models created from data composed of physical compositions and proximate or elemental analysis of MSW [15–18]. The chemical entities in waste represent the local properties, whereas the heat value or combustion rate of the waste represents the global properties. The global properties can be estimated using a homogenization analysis, where the macro properties of a heterogeneous medium are studied by averaging over its local properties [19,20]. The oxidation of carbon, nitrogen, hydrogen, sulfur, and other elements in waste are local energy conversions, whereas the total combustible content is the global energy conversion, i.e., the sum over the averaged local energy conversions.

The energy content of MSW can be described as the lower heating value (LHV), expressed as the higher heating value of the ash and moisture free waste—also called HHV_{awf}—minus the latent heat of evaporation of moisture

$$LHV_{aw} = HHV_{awf}(1 - M_w) - L_v M_w \quad (1)$$

where M_w is the fractional moisture content and L_v is the latent heat of the vaporization of water [18]. Equation (1) is based on homogenizing waste compositions into three components: combustible, moisture, and ash. The LHV estimations can be used for assessing the self-sustained combustibility. The self-sustained combustibility can also be assessed by using graphical plots of the ash, moisture, and combustible content in the Tanner diagram [21]. Moisture content variations in waste dominate over the variations in ash and combustible content in increasing or decreasing the LHV. Therefore, moisture is an important parameter for assessing the heating value of MSW. The LHV of MSW can also be assessed by characterizing specific waste fractions with corresponding LHVs [22–26]. LHV estimation based on waste fraction compositions requires a preanalysis of the global properties (moisture, ash, combustibles) of waste components such as food, organic waste, plastic, textiles, paper and cardboard, leather, rubber, wood, metals, glass inserts, and fines.

2.1.2. Combustion Rate

Another important factor for the incineration processes is the local shape and size properties of the waste compositions. The surface-area-to-volume ratio of waste is a local parameter that influences the combustion rate of materials [27]. Local properties of waste features such as pore, channel, and particle size can be homogenized into a global parameter such as air permeability to estimate the combustion rate. Air permeability depends on moisture content, hydrophilicity, compressive modulus, and compressive strength of waste materials and can be used for estimating combustion rate for common waste fractions [28–30].

2.1.3. Problematic Materials

Waste materials that result in dangerous flue gases containing heavy metals; increased emissions of CO, NOx, or SOx, acid gas, and gas particulates; or degradation of the WtE facility, such as corrosion of the grating, are problematic for the energy recovery process [31,32]. Some waste materials can also pose health and safety risks at the WtE plant [33]. Local properties of problematic waste include chemical entities such as halogenated solids or liquids,

heavy metals, high concentration of polysaccharides, fatty or amino acids, flame retardants, water, and ash minerals [31,32]. Global properties of problematic waste consist of oversized objects, compressed canisters or gas cylinders, high moisture content, high ash content, low combustible content, and low combustion rate [15,31–33]. The characterization of problematic materials in MSW requires assessment of both the local and global properties.

2.2. Impact of Heating Value and Combustion Rate of Waste on the Incineration Process

The incineration processes are generally controlled based on manipulating the variables of feeding rate, primary and secondary air flow, and grate speed transporting waste through the different drying, pyrolysis gasification, oxidation, and burnout zones [15]. A proportional–integral–derivative (PID) model is often used as a control strategy where the manipulated variables are coupled in loop with the measured steam and oxygen flow of the system. A schematic of a PID controller is shown in Figure 1.

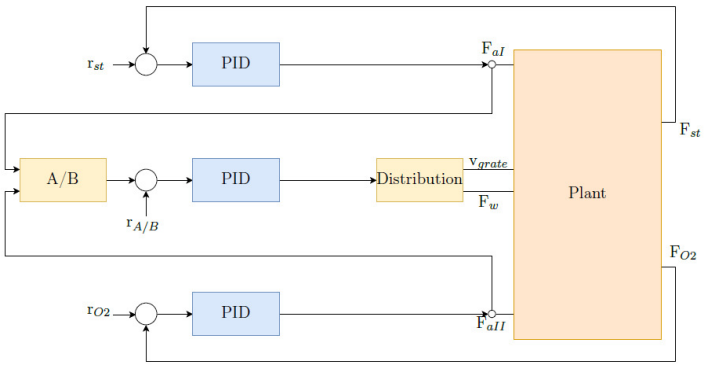

Figure 1. Schematic of a PID controller for waste incineration (adapted from [34]).

In Figure 1, r_{st} and r_{O2} are the desired set-points for steam and oxygen flow, respectively, and $r_{A/B}$ is the desired set-point of the ratio between primary air flow F_{aI} and secondary air flow F_{aII}. With an increase in LHV, the steam flow F_{st} will increase due to higher flue gas temperature heating up the boiler; meanwhile, oxygen flow F_{O2} will decrease due to higher demand for oxygen in furnace. The PID-controller response to the increase in steam flow and decrease in oxygen flow is a decrease in primary air flow, an increase in secondary air flow, and an increase in feeding rate F_w and grate speed v_{grate}. As a consequence of the increase in feed rate and grating speed, the PID controller will further increase the steam flow and reduce the oxygen flow. The coupling between steam production increase and oxygen reduction with the increase in feed rate and grating speed are compensated by the primary airflow controller reducing its output and the secondary airflow controller increasing its outputs. Similarly, with a decrease in LHV, the steam flow decreases and oxygen flow increases. The PID-controller will then increase primary oxygen flow, reduce the secondary oxygen flow and decrease feeding rate and grating speed. The decrease in feeding rate and grating speed will further result in a steam flow decrease and oxygen increase. The primary and secondary airflow controllers will increase and decrease their outputs, respectively, to compensate for the coupled process between steam production and oxygen flow with feeding rate and grating speed [35,36]. In addition, large changes in combustion rate will enhance the effect of high or low LHV on the PID-controller. Large variations in LHV and combustion rate outside the PID controller's operating boundaries would result in an unstable incineration and require a more intense supervision of the process by the plant operators.

3. Literature Review: Sensor Technologies for Waste Monitoring

A sensor is a device composed of a transducer and a recognition element. The sensor recognizes parameters such as force, temperature, pressure, ionic strength, or pH, which are converted into a signal by a transducer that is either electrical, optical, or mechanical.

Different sensor techniques can be classified according to operation in contact, in proximity, or in remote settings. In a WtE plant, sensor systems can potentially measure parameters used for estimating fuel quality values that, in turn, can be used as feedforward for process control or implemented as indicators for process alarms. Fuel quality values can contain information about problematic waste material contents, the lower heating value, or the combustibility. In operation, the information from sensor systems can help to remove problematic waste materials, perform specific mixing of waste materials to improve the homogenization, select specific waste to the incinerator, or used for control incineration parameters. In the following sections, an overview of sensor categories most relevant for waste monitoring and their fundamental operating principles are presented. The fundamental operating principles of the sensor techniques are needed to evaluate their utilization potential for monitoring applications relevant for identifying and quantifying fuel quality parameters of MSW to increase the WtE performance.

3.1. Photonic Sensors

Photonic sensors operate in the ultraviolet (UV) from 10 nm to 400 nm, visible (VIS) from 400 nm to 700 nm, or infrared (IR) from 700 nm to 1 mm wavelength range. The IR domain is usually divided into subregions; near-infrared (NIR) from 700 nm to 1400 nm, short-wavelength infrared (SWIR) from 1400 nm to 3000 nm, mid-wavelength infrared (MWIR) from 3000 nm to 8000 nm, long-wavelength infrared (LWIR) from 8000 nm to 15 µm, and far-infrared (FIR) from 15 µm to 1 mm wavelength. The FIR domain is often defined in the frequency domain instead of the wavelength domain, i.e., from 300 GHz to 20 THz. The amplitude, wavelength, phase, and polarization of the electromagnetic (EM) wave can be used for sensing. For common applications such as imaging and spectroscopy, the amplitude and wavelength parameters are used. EM waves interact with materials through an energy exchange with its electronic or molecular vibrational and rotational transitions. The different types of energy exchange events result in reflection, diffraction, scattering, and absorption in materials. In the IR domain, the energy of photons corresponds mostly to the vibrational and rotational energy transitions, whereas for absorption in the UV–VIS domain, the energy of the photons corresponds mostly to electron energy transitions [37]. Since the photon energy of UV–VIS and IR corresponds to different types of energy transitions, the use of different wavelength domains in sensor techniques provides different type of information about specific materials. By heating and atomizing materials, the electronic transition energy itself can also be used for detecting the spectral signatures of emitted light from elemental compositions. A highly energetic beam such as short laser pulses incident on materials can heat up and atomize the sample such that a localized plasma plume is created. The localized plasma plume consists of electronically excited atoms and ions that will decay back to the ground state after the duration of the laser pulse. The decay in atoms and ions from the plasma-induced excited state to ground state emits characteristics wavelengths of light. The characteristic wavelength of the light have a photon energy equal to the energy difference between the higher and lower electronic state that is unique to each element heated and atomized by the short laser pulse [38].

For reflection and transmission in bulk materials, the light–matter interaction can be described by the refractive index for different wavelengths. For an isotropic medium, the complex refractive index can be expressed as

$$\tilde{n}(\lambda_0) = n(\lambda_0) - j\kappa(\lambda_0) \tag{2}$$

$n(\lambda_0)$ and $\kappa(\lambda_0)$ can be measured experimentally and used to estimate phase velocity, attenuation ($\kappa < 0$), or gain ($\kappa > 0$) of light propagating in a medium [37]. For normal incidence, the reflectance $R(\lambda_0)$ at an optically flat interface between two materials (material 1 and 2) is given by the Fresnel equations,

$$R(\lambda_0) = \left| \frac{\tilde{n}_1(\lambda_0) - \tilde{n}_2(\lambda_0)}{\tilde{n}_1(\lambda_0) + \tilde{n}_2(\lambda_0)} \right|^2 \tag{3}$$

where $\tilde{n}_1(\lambda_0)$ and $\tilde{n}_2(\lambda_0)$ are the complex refractive index for mediums 1 and 2, respectively [37]. The transmittance $T(\lambda_0, d)$ of a plane EM wave traveling through a medium with depth d is given as

$$T(\lambda_0, d) = |\exp(-j\tilde{n}(\lambda_0)k_0 d)|^2 \quad (4)$$

where k_0 is the vacuum wavenumber [37].

Particles or chemical entities in a (lossless or lossy) homogeneous medium cause additional absorption and scattering. The resulting transmittance for isotropic heterogeneous mediums can be described by Lambert–Beer's law,

$$T(\sigma_{ext}, d) = \exp(-\sigma_{ext}\rho d) \quad (5a)$$

$$\sigma_{ext}(\lambda_0) = \sigma_{sca}(\lambda_0) + \sigma_{abs}(\lambda_0) \quad (5b)$$

where $\sigma_{ext}(\lambda_0)$ is the extinction coefficient, $\sigma_{sca}(\lambda_0)$ is the scattering coefficient, $\sigma_{abs}(\lambda_0)$ is the absorption coefficient, and ρ is the number density of particles or chemical entities. For chemical entities, the term $A = -\sigma_{ext}(\lambda_0)\rho d$ can be expressed in terms of molar absorptivity ε_a and concentration c as $A = -\varepsilon_a c d$ [37]. For spherical particles, the scattering and extinction coefficient are given by the Mie Theory, whereas for spheroidal particles, the coefficients are given by Gans theory, a generalization of the Mie theory [39–41].

In the UV–LWIR wavelength region, the penetration depths are short in most solid materials such that only reflectance is of interest [10,42–46]. For LWIR–FIR, the penetration depth is longer in most materials and both reflectance and transmittance measurements can be performed. The exception is water and metals where the penetration depth is short [47]. Reflection and transmission of light in materials can be specular or diffusive. Diffusive reflection and transmission are a result of surface roughness or multiple light scattering within the material.

The identification, or characterization, of specific materials can be determined with single-point spectroscopy measurements [42–45]. Spectral imaging, either multi- or hyperspectral, for the UV–SWIR wavelength domain can also be used [10,46]. The differentiation and detection of specific materials is possible due to the materials exhibiting different complex refractive indices and scattering and absorption cross-sections. Imaging in the MWIR–LWIR wavelength domain is limited to detection of thermal radiation. Different materials, at the same temperature, emit different thermal radiation intensities that can be differentiated using MWIR–LWIR imaging [48]. MWIR–LWIR imaging can be performed with or without an illuminating source. Without an illuminating source, elevated sample temperatures are often necessary for material characterization. For FIR, the light interaction with materials' compositions are dominated by high reflection from metals and high absorption in water, thus enabling specific detection of these respective components. For other materials, the light–matter interactions in this wavelength range will normally be dominated by scattering effects of material particles with dimensions on the order of the wavelengths [47].

The photonic sensors are presented in Sections 3.1.1–3.1.3, where we focus on general applications of photonic devices for MSW characterization limited to use of external light sources and detectors without contact with the samples and without pretreatment of the samples. This limits the relevant photonic sensors to single-point spectroscopy techniques in the UV–LWIR wavelength domain, to multi- or hyperspectral imaging in the UV–SWIR wavelength domain, and to THz spectroscopy in single-point or imaging measurements.

3.1.1. Single-Point Measurements in the UV–LWIR Wavelength Domain

Single-point MSW characterization with UV–LWIR spectroscopy uses either the reflected or transmitted light spectrum averaged over an area or volume of the sample within the acceptance cone of the optical system [43,49]. For the NIR–LWIR wavelength domain, the detector and the light source consist of semiconductor alloy systems (either II–VI- or III–V-based alloys) and are mostly used for specialty applications such as measuring specific gas molecules or remote monitoring of agriculture [37]. For NIR–SWIR, many

components are used for telecommunication applications and are available at low costs. For SWIR–LWIR, there are no high-volume applications and the light sources and detectors used are often expensive. For the UV–VIS wavelength domain, the detector is silicon-based, such as in charged couple devices (CCD) or complementary metal-oxide semiconductors (CMOS), and are used in common devices such as cameras on smartphones or digital single-lens reflex cameras. The light source in UV–VIS consists either of incandescent light or semiconductors based diodes or lasers that are designed for emitting certain wavelengths with a limited bandwidth and are used in most infrastructure light settings. The availability of light sources and detectors used in the UV–SWIR wavelength domain result in low manufacturing costs for the sensors. Light spectrum measurements can be performed either by tuning the wavelength of the light source or by using a broadband light source combined with a dispersive optical element with scanning slits behind the light source or in front of the detector. Instead of scanning slits, an image sensor can be used where each pixel measures photon count for each wavelength dispersed by an optical component [37].

Single-point waste material monitoring with UV–LWIR spectroscopy sensors are mostly based on either laser-induced breakdown spectroscopy (LIBS) or absorbance spectroscopy. With LIBS, a highly energetic light beam is focused on the sample to generate plasma and ionized matter that excites electronic transitions and spectral signatures of chemical compositions in a solid, liquid, or gas state. The energetic light beam is created by using pulsed light. The detection of emitted wavelengths from the sample are normally in the UV–NIR range [38]. Typical waste materials detected with LIBS are halogenated plastic or polymers [42]; metal scraps such as Fe, Cr, Ni, Mn, Mo, Cu, Si [50]; and industrial plastics such as polyethylene terephthalate (PET), high-density polyethylene (HDPE), polyvinyl chloride (PVC), light-density polyethylene (LDPE), polypropylene (PP), and polystyrene (PS) [51]. With absorbance spectroscopy, a light beam is focused on the sample and the transmitted or reflected light is measured relative to the incoming light intensity. Specific light wavelengths with different energies will correspond to specific energy transitions and result in characteristic absorbance dips in the transmittance or reflectance spectra [52]. For MSW monitoring, absorbance spectroscopy is mostly performed in the NIR and less in the SWIR–LWIR and VIS wavelength domain. For NIR, waste materials detected by multiple studies are PET and PVC [49]; PET, HDPE, PVC, PP, and PS [43]; carbohydrate, nitrogen, and lipids [53]; organic waste [54,55]; and oil-contaminated cardboards [56]. For SWIR–LWIR, industrial plastic waste can be detected such as PET, polyethylene (PE), PP, PS, polylactic acid (PLA), HDPE, and LDPE [44]. For VIS, PP resins have been detected based on color measurements [57].

3.1.2. Imaging in the UV–SWIR Wavelength Domain

For MSW characterization with UV–SWIR imaging, the reflected light from a material is spectrally and spatially resolved. Each pixel in the image contains information about photon intensity for multiple wavelengths [10,58]. Due to the vast amount of information obtained with spectral imaging, this technique can be effectively used with supervised or unsupervised machine learning methods for classification and linear regression analysis to identify or quantify specific materials [59,60]. Image sensors for the UV–SWIR wavelength domain are based on detectors mentioned in Section 3.1.1. To obtain spectral information, there are three methods commonly used: mosaic color-filter adhered on image sensors, color-filter wheel in front of the image sensor, and the push-broom scanner in front of the image sensor [61,62].

Waste monitoring with UV–SWIR imaging techniques has mainly been focused on hyperspectral (20–200 wavelength bands), multispectral (3–20 wavelength bands), and RGB (3 wavelength bands) or monochrome cameras. RGB and monochrome camera have also been used for 3D imaging, RGB color imaging, or for human intervened image analysis for recognizing different type of fractions in MSW. With monochrome 3D imaging, the shape and volume of waste can be estimated [63]; with RGB color 3D imaging, particles, plastic, and metals can be detected [64]; with RGB color camera with human intervened imaging

analysis, paper, card plastic, film plastic, dense plastic, wood, glass, organics, metals textile, waste electrical and electronic equipment (WEEE), and inerts can be identified and quantified [24,25]. Hyperspectral and multispectral imaging of MSW are used over the whole UV–SWIR wavelength domain. Considering manufacturing cost, the imaging in the UV–NIR band uses detectors at lower costs compared with detectors used for imaging in the NIR–SWIR band. However, spectral imaging in the NIR–SWIR band results in higher specificity in detecting materials compared with the UV–NIR, due to the overtones and combination tones found in this spectral region.

UV–VIS–NIR-domain-based hyperspectral camera can detect waste materials such as poly(methyl methacrylate) (PMMA), acrylonitrile butadiene styrene (ABS), polycarbonate (PC), PVC, rubber, PE, PP, and particles [65]; polyefins, wood, foam, and aluminum [46]; or biosolids [10]. In the VIS–NIR, hyperspectral techniques have been used for identifying fine particles, electronic waste, and components such as CuZn, Fe, Cu, Al, and Ni [66]. For hyperspectral imaging in the NIR–SWIR domain, it is able to detect plastic and nonplastic waste [67,68]; moisture [58]; and raw cardboard, colored cardboard, newspaper, and printed paper [69]. The identification of waste classes for general properties of waste has also been demonstrated on a WtE plant using multispectral imaging in VIS–NIR with deep learning methods [14].

3.1.3. Single Point and Imaging with THz Techniques

THz sensor system architectures can be configured for spectroscopy measurements for single-point detection or for imaging. Measurements can be performed in the frequency domain or in the time domain. For the frequency domain, measurement of the reflected or transmitted light intensities over the sample result in contrast differences related to certain materials such as metal or water. In the time domain, THz pulses are used. The reflected or transmitted pulse amplitude and phase are measured as a function of time, followed by a fast Fourier transformation to transform the amplitude–time measurements to the frequency domain.

MSW characterization using THz is focused on moisture content detection in solid materials. Applications also include nondestructive testing in the print industry, building materials, biomass, plant cultivation, soil monitoring, or monitoring of oil–gas reservoirs. For the frequency-domain, intensity measurements of moisture content in wood [70,71], biomass [11], concrete [70,72], and paper [45] have been performed, whereas for THz imaging, moisture content in leaf [73], soil [74], wood [71], and biomass [11] have been measured. THz time-domain spectroscopy measurements have been performed to detect moisture in rapeseed leaves [75], paper [76], polyamide and wood plastic composites [77], food wafers [78], and active carbon pores [79]. For THz imaging with time domain spectroscopy, moisture content in paper [76] and polyamide and wood plastic components [77] have been measured.

3.2. Radiowave Sensors

Radiowave sensors use frequencies lower than the FIR frequencies used for the photonic sensors. Thus, the radiowave domain starts at 300 GHz and goes as low as 3 kHz. Generation and detection of radiowaves are performed using antennas with a transmitter or a receiver [80]. Sources used include FET, Gunn, or IMPATT diodes based on solid-state devices for low power, or a magnetron based on EM-controlled motion of electrons in vacuum [81] for high power. To obtain optimum power transfer between the source or detector and free space, impedance matching is needed using components such as feed-horns. The horn-antenna provides a gradual transition structure to match the impedance of the microwave source or the detector to the impedance of free space as well as directing or collecting the radiation [82]. Radiowave interaction with materials can be described by the complex refractive index in (2), as in the photonic domain, Fresnel equation in (3), wave propagation in (4), and Lambert–Beer law in (5a). For mediums with magnetic permeability included, the radiowave transmission can be attenuated, but this effect is not included in the expressions used.

The radiowave–matter interactions are dominated by water absorption and metal reflection, as for light in the FIR wavelength domain, due to long wavelengths with photon energies lower than most molecular energy transitions in materials. This results in high transmittance of radiowaves in most materials except water and metals. The high attenuation in water is due to excitation of rotational energy transitions of the water molecules. The high reflection in metal is a result of the strong interplay between the EM wave and the high density of the electrons in metals. For other materials, interactions between EM wave and electrons are weaker and lead to low reflections [83]. Radiowave reflectance or transmittance measurements can be used for detecting moisture or metal content in materials. These measurements are often conducted as single-point spectroscopic measurements. Radiowave imaging can also be performed, but the images obtained will have a low resolution due to the long wavelengths used in this domain.

Radiowave sensors related to characterizing MSW properties are mostly based on permittivity measurements [84] or on open-ended coaxial line probes (OECP) measuring broadband dielectric properties [85]. For microwave techniques, not used in contact with the sample, the transmittance measurements can be performed for frequencies between 2 GHz and 135 GHz. Either moisture content or dielectric properties can be measured in various materials. Dielectric properties have been measured on granular matter such as wheat, corn, and soybean [86] or biodegradable waste [87]. Moisture content has been measured in granular or particulate materials [88], pellet biomass [89], or mixed MSW [26]. The OECP techniques must be performed in proximity to the sample and can obtain dielectric measurements for frequencies between 30Hz and 15 GHz. Dielectric properties have been measured for general material types [90] and heterogenic and dispersive clay materials [91]. Moisture content has also been measured with OECP techniques for sawdust [92].

3.3. Electric and Magnetic Sensors

Electric or magnetic sensors are electronic devices that can be used for measuring a physical quantity, e.g., pressure, strain, compression, temperature, and magnetic or electric fields [93]. This section mainly focuses on the use of capacitance, resistivity, time-domain reflectrometry (TDR), and inductance to detect moisture or metal in MSW.

Capacitance sensors are based on detecting the electric charge of a system relative to the corresponding difference in electrical potential. Capacitance can be described as

$$C = \frac{Q}{|\Delta V|} \tag{6}$$

where Q is the amount of charge stored in a capacitor and $|\Delta V|$ is the potential difference between the conductors [93]. Capacitance sensors can be based on a parallel-plate capacitor consisting of two parallel plates with area A separated by a distance d. With a dielectric material between the plates, the dielectric permittivity is given by $\varepsilon = \varepsilon_r \varepsilon_0$, where ε_r is the relative permittivity. Gauss law can be used with (6) to find the electric field of the charge distributions and the capacitance for the parallel-plate described as [93]

$$C = \frac{\varepsilon A}{d} \tag{7}$$

The dielectric can change as a function of a change in moisture in materials. Increasing water content increases ε, which leads to an increase in capacitance. The capacitance can also increase due to an increase in metal content. For increasing metal content, the dielectric medium will, after a threshold value, become conductive and short-circuit the capacitor. As seen from (7), capacitance is also inversely proportional to the distance, which limits the capacitive sensor to operate in proximity to the sample. The moisture content of waste has been estimated in proximity to the sample measuring the complex impedance and capacitance [94].

Resistivity sensors are based on detecting the change in current through a conducting sample as a function of change in the resistivity of a material due to changes in moisture. Resistance of a conductor is described as

$$r = \frac{\rho l}{A} \tag{8}$$

where ρ is the resistivity, l is the conductor length, and A is the cross-sectional area of the conductor [93]. The most conventional method to perform resistivity monitoring is by inserting two or more electrodes in a sample to measure the resistivity as a function of material composition. Increasing water content in materials decreases the resistivity, and the resistance is measured from the relation in (8). Resistivity detection is a contact method since electrode probes are required to be inserted into the sample material to monitor resistivity. By using a multielectrode principle for electrical resistivity tomography, the moisture content has been detected in soil in field experiments [95]. For MSW, moisture content has been estimated by performing resistive measurements using two electrodes in a granular matrix [96].

TDR sensors are based on transmitting a pulse along conductors while measuring the reflection as a function of the impedance differences in sample materials. Thus, TDR sensors are similar to resistivity sensors as they require insertion of conductors to perform resistance or impedance measurements and similar to radar or OECP since they perform reflection measurements from the EM pulses transmitted along the conductors. The travel time for the pulse to propagate the length of the conductors and back is a function of the dielectric permittivity of the sample material and can be described as

$$t = \frac{\sqrt{\varepsilon} 2L}{c} \tag{9}$$

where t is the travel time of pulse, L is the length of the conducting probes, ε is the effective dielectric permittivity of the sample, and c is the speed of light [97]. For materials with an increase in moisture content, the dielectric permittivity will increase and result in a larger travel time of the pulse propagating along the conducting probes. The use of wave propagation along a three-rod probe has been used for estimating moisture content, metal, or salts in agri-food materials [98] or moisture content and density in unbound road materials [99] from electrical permittivity measurements.

Inductive sensors are based on generating and detecting magnetic flux by using inductive coils. The sample can be considered as a slab where a sender is located on one side and a receiver located on one of the sides. The sender or transceiver coil is used for projecting a magnetic flux onto the sample while a receiver coil is used for measuring the magnetic flux generated from the sample. The magnetic flux from the sample is a result of the eddy current induced by the incident magnetic flux. The magnetic flux density B is a function of the magnetic field strength H and is used for finding the magnetic flux ϕ by integrating over the enclosed surface area

$$\phi = \int_S B \cdot dA \tag{10a}$$

$$B = B_i + B_e \tag{10b}$$

where S is the enclosed surface area, A is the area of the magnetic flux incident on sample, B_i is the imposed magnetic flux density on the sample, and B_e is the induced magnetic flux density of the eddy field in the sample [94,100]. By using Maxwell equations, the eddy current created by the charges in motion can be solved for a one-dimensional slab as

$$J(x) = -\frac{jkB_i}{\mu_0} \frac{\exp(jkx) - \exp(-jkx)}{\exp(jkd) - \exp(-jkd)} \tag{11}$$

where $k = \sqrt{-j\omega\sigma\mu_0} = q - jq$ is the complex wavenumber at low frequencies, ω is the angular frequency, σ is the electrical conductivity, μ_0 is the magnetic permeability in free space, d is the thickness of the slab, and x is the position along the thickness of the slab. The exponential component $\exp(jkx)$ in (11) can be rewritten for real and imaginary components with $q = \sqrt{\omega\sigma\mu_0/2}$ into $\exp(qx)\exp(jpx)$ to define the decay length $1/q$ as the skin depth [94,100]

$$\delta = \sqrt{\frac{2}{\omega\sigma\mu_0}} \tag{12}$$

As seen from (12), the skin depth of the magnetic flux will be highly dependent on material compositions containing metals since it is inversely proportional to electrical conductivity σ. By inducing eddy currents for different angular frequencies, different entities with different electrical conductivities can be detected and differentiated in a mixed material composition. Magnetic inductance spectroscopy has been used for measuring real and imaginary components of the magnetic field to classify different nonferrous materials in waste [101]. Inductive transceiver and receiver coils for single-frequency generation and detection of magnetic fields have been applied for detecting metal in waste [12,102], the detection and counting of ferrous and nonferrous particles [103], and sorting of nonferrous metals [104,105].

3.4. High-Energy Particle Sensors

Photons are also understood as stable particles with no electric charge and no mass, but with momentum and magnitude relative to the energy of the particle. Therefore, in this section, high-energy photon sensors are categorized in the same class as high-energy particle sensors. High-energy particle sensor systems use signal excitation sources in an energy domain that are sufficiently high for ionizing materials or for stimulating nuclear radiation emissions [106,107]. High-energy particle sensor systems used for MSW characterization include X-ray techniques and neutron sensor probes [4,6].

X-rays are EM waves, such as light or radiowaves, but interact differently with matter due to their high photon energy. Generation of an X-ray is achieved by applying high voltage to a vacuum tube or X-ray tube. Detection of an X-ray is performed by using a charge collector plate for detecting the X-ray and an image sensor for imaging the charge collection [107,108]. The wavelength domain of X-rays is between 10 nm and 0.01 nm, with energies corresponding to ionizing energy transitions in atoms. X-rays interact with matter through photoabsorption, Compton scattering, and Rayleigh scattering [107,108]. Photoabsorption occurs as a result of X-ray radiation having an energy equal to or greater than the binding energy of an electron in an atom. The X-ray photon is entirely absorbed by the electron in an atom and the electron is ejected with a kinetic energy equal to the X-ray photon. The ejected electrons are called secondary electrons. Ejection of electrons from the inner orbitals create an unstable electron structure of the atom and result in electron relaxation to fill the hole of the ejected electron. The relaxed electron emits a photon energy equal to the energy difference between the two orbitals involved in the electron relaxation [107,108]. For Compton scattering, an interaction occurs between the photon and electrons in the outer orbital. This scattering process is inelastic, where the energy of the photon is partially absorbed by the outer orbital electron resulting in electron ejection. The kinetic energy of the ejected electron is equal to the energy difference of the photon before and after the Compton scattering [107,108]. Rayleigh scattering is an elastic scattering process where the photon is absorbed and re-emitted by the electron cloud of the atom resulting in no ionization or energy transfer between photon and electron [107,108].

The photon energy range of X-rays is divided into two domains, where one domain includes soft X-rays with wavelengths higher than 0.1–0.2 nm [108,109] and the other domain includes hard X-rays lower than 0.1–0.2 nm [108,110]. Hard X-ray has a wavelength with dimensions similar to atoms and scatters efficiently in periodic structures below one nanometer; it also has a high penetration depth in many materials. Soft X-ray has high

attenuation in most materials and ambient air with a photon energy corresponding to binding energies of electrons of different elements in materials. The attenuation for soft X-ray is mostly dominated by photoabsorption, whereas for hard X-ray, the interaction with matter is mostly dominated by Compton scattering. The Rayleigh scattering events, however, are small for both hard and soft X-rays [108–110].

The use of soft and hard X-rays for MSW characterization provides different information about materials related to elemental composition or density. Reflection measurements with soft X-ray can be used for elemental composition analysis since the photoabsorption and relaxed electron-induced X-ray emission is highly dependent on the atom number of an element. Transmission measurements with hard X-ray are used for density analysis of certain materials since the Compton scattering in combination with photoabsorption is highly dependent on the ion or electron density of material compositions. Earlier work found in literature related to MSW characterization were based on imaging or spectroscopy with dual-energy X-ray transmission (DE-XRT) or X-ray fluorescence (XRF). X-ray fluorescence is a technique based on photoabsorption of soft X-ray in materials where the energy or wavelength difference between the excitation and emitted X-ray is measured and used for characterizing elemental compositions in a sample [111]. DE-XRT is a technique based on using dual emission of hard X-ray incident on the sample with different energies or different wavelengths [112]. The attenuation of dual hard X-ray with different wavelengths results in a difference in the transmission intensities related to the density differences in a material. DE-XRT has been used for detecting and differentiating nonferrous metal in waste [13], waste fraction by density [4], or cast and wrought aluminum [4]. For XRF measurements, metal, plastic, and wood have been detected in waste [4]; retardants in polymers and inorganic preservatives, arsenic contaminant, or moisture in wood [6]; and primary raw materials in waste [113].

Neutron sensor probe is a moisture meter technique based on neutron particle emission in materials. The neutron probe consists of a sealed metallic cylinder that contains a neutron detector and a radioactive source emitting fast neutrons. The neutron sensor probe is in contact with materials through an access tube that is protecting the probe [114,115]. The radioactive source emits high-energy neutrons into the surrounding medium creating a neutron particle cloud. The high-energy neutron particles in the cloud are more likely to reflect and scatter in materials with light atomic weight elements such as hydrogen than in those with high atomic weight elements. The interaction of the fast neutrons with light atomic weight elements slows the neutrons to thermal or slow neutrons [114,115]. The scattered slow neutrons are then detected and counted by a gauge in the neutron probe. The equilibrium changes between the fast and slow neutron particle clouds in materials can then be directly measured as a function of the amount of hydrogen or water content. A calibration curve must be established to relate the measurements of thermalized neutrons to the volumetric water content in materials [114,115].

The interaction volume of the neutron particle cloud has been found to have a radius of 150 mm in wet soil and 700 mm in dry soil [116]. The macroscopic sampling around the neutron sensor probe can then potentially be used for representing volumetric moisture measurements in heterogeneous MSW materials. The moisture measurements with neutron probe sensor are, however, not without cross-sensitivity issues. Hydrogen can be bound in materials such as clay, wood, or plastic materials and will increase the count ratio of thermal neutrons for constant moisture content [117]. Another cross-sensitivity issue is the neutron capture effect. Thermalized neutrons are subject to capture for many elements. Elements in MSW that capture slowed neutrons are iron, potassium, and chloride and will decrease the count ratio of thermal neutrons for constant moisture content [117]. Due to the bound hydrogen and neutron capture effect, the change in density of MSW would also change the slow neutron count rate. Despite these cross-sensitive effects, neutron sensor probes have been shown to perform well for moisture measurements, not only for soil materials but also for MSW. Laboratory experiments have been performed to measure hydrogen content in waste with neutron sensor probes as an indicator in estimating the quality of waste fed

to the incinerator [118]. In other work, laboratory and field experiments were performed, where moisture content was measured in MSW landfills with neutron sensor probes [117].

4. Material and Methods

4.1. Framework for the Assessment of MSW Sensor Technologies

The sensor techniques presented in Section 3 will be assessed in terms of the WtE process plant design and framework of use as follows: (1) the incineration design is based on the use of grabbing cranes to transport the waste to the feeder of the incinerator [23,119]; (2) the process design does not use shredding or magnets to process the waste prior to incineration, i.e., the waste is bulky and is received "as is" from the municipal waste management suppliers [23,119]. The feasibility assessment is mainly focused on the adaptability, versatility, specificity, and sensitivity of the different monitoring techniques. Adaptability and versatility of sensor techniques are important for their impact in assessing the fuel quality parameters. In general, a multimodal sensor system is preferred since monitoring of multiple features in waste materials can be used to represent multiple different estimates of the fuel quality. The assessment is initialized by categorizing the sensor techniques for contact, proximity, and remote settings to elucidate the compatibility of the sensor methods and the framework used for the WtE process plant.

4.2. Measurement Modes Used by MSW Sensor Methods

Sensors can operate in transmissive or reflective settings. A transmissive measurement in this assessment is based on using a transmitter and detector, as shown in Figure 2a. For the reflective method, the transmitter and detector are located on one side of the medium, as shown in Figure 2b.

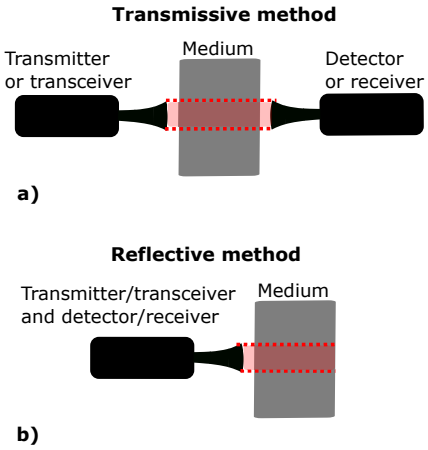

Figure 2. (**a**) Illustration of transmissive method. (**b**) Illustration of reflective method.

Using the measurement modes shown in Figure 2, the performance of potential sensors techniques based on their fundamental operating principles are evaluated.

4.3. Assumptions Used for Computing Reflectance and Transmittance Changes to Moisture for Radiowave and THz Frequencies

The use of radiowave or THz techniques for moisture measurements can be assessed from estimations using (4) for transmittance and (3) for reflectance. The use of such simple models represents near-ideal monitoring scenarios with the following assumptions applied: (1) metal content is omitted; (2) the structures of the waste material components are much smaller than the wavelength of EM waves so that scattering effects can be neglected; (3) the variations of refractive index of waste materials is much smaller than the variations of the bulk refractive index as a function of moisture content; (4) the waste medium is homogenized with effective refractive index as a function of the volume fraction of waste and water. We note that assumption (2) is rarely satisfied in the THz domain since

wavelengths are in the dimension of 10 μm to 1 mm and will scatter from waste structures with the same dimensions. Assumption (3) is equivalent to assuming that the refractive index of waste materials (without water) is approximated to 1.

With these assumptions, we can estimate the ideal signal intensities for water volume fractions and waste sample lengths as well as ideal intensity contrasts between low and high water contents. The effects of metals, scattering processes, and waste material refractive indexes will result in smaller signal intensities and lower intensity contrast between high and low water contents. The complex dielectric values to be used with (4) and (3) of waste materials with moisture can be estimated by using effective medium approximations. This approximation uses volume averaging of refractive indexes, $\tilde{n}_{\text{eff}}(\lambda_0) = v_{wm}\tilde{n}_a(\lambda_0) + v_{wt}\tilde{n}_b(\lambda_0)$, where $v_{wm} = 1 - v_{wt}$ is the volume fraction of waste materials with complex refractive index $\tilde{n}_a(\lambda_0)$ and v_{wt} is the volume fraction of water in waste materials with complex refractive index $\tilde{n}_b(\lambda_0)$ [120]. The complex refractive index of moisture $\tilde{n}_b(\lambda_0)$ can be found from experimental measurements performed by [121].

4.4. Performance Parameters Used for Assessing Implementation of MSW Sensor Indicators

The input parameters for process control and process alarms impose different demands on sensor technique qualities in terms of dynamic range, specificity, and sensitivity. Dynamic range is the highest and the lowest amount of an entity that is possible to be measured. Sensitivity is the smallest change in the amount of an entity that is possible to be detected. Specificity can be viewed as the possibility for a measurement to be sensitive to one entity only. For process control, a sensor method with high specificity and sensitivity is desired. With high specificity and sensitivity, it is possible to produce a small value change in fuel quality estimations that is valid for a wide range of different waste material compositions. The dynamic range of the fuel quality measurements must be within a domain relevant for the boundary conditions used by the process control. In addition, if sensor parameters should be included as a forward loop in the process control, the time has to be known between the waste monitoring event and the waste incineration event. For process alarms, there are less demands on sensor dynamic range, specificity, and sensitivity. It is the holistic quality of a sensor method that is important to evaluate its ability to produce alarms with acceptably low levels of false positives and negatives. It is perhaps more important for a measurement to be performed within the dynamic range required to initiate an alarm on fuel quality values. For a large increase or decrease in fuel quality parameters, alarm indicators may be be used to assist the operative control of the incineration.

5. Results and Discussion

5.1. Remote, Proximity, and Contact MSW Sensors

Contact sensors, including resistivity sensors, time-domain reflectrometry (TDR) sensors, and neutron particle probe sensors, can only be operated when embedded into the waste samples. Proximity sensors, including open-ended coaxial line probe (OECP) radiowave sensors, X-ray sensors, capacitance sensors, and inductive sensors, must operate in near-contact with the waste samples. Remote sensors, including ultraviolet (UV) to long-wavelength infrared (LWIR) spectroscopy, UV to short-wavelength infrared (SWIR) imaging, THz spectroscopy and imaging, as well as radiowave permittivity measurements, can be operated with variable distances to the waste samples.

For the process design considered here, contact sensors can only work in an offline setting where waste samples are transported into a separate and independent stream of the process so the insertion of sensor probes can be controlled. Due to the challenge in integrating fuel quality indicators from offline settings to the process control system, contact sensors are the least adaptable technique for monitoring in the waste-to-energy framework. Proximity sensors are able to operate in online settings. Scans over waste samples can be performed using conveyor belts for controlled waste transport. Proximity sensors show great potential for specific and sensitive detection of moisture, metal, plastic, and wood, as presented in Sections 3.2–3.4. Remote sensors also operate in online settings and can

be adapted for different waste monitoring locations with variable monitoring distances to waste samples. The wide spectral range used by the remote sensors enables the detection of a wide range of materials, as presented in Sections 3.1 and 3.2. The main criteria for further consideration of potential sensors is the possibility for online monitoring. Thus, only remote and proximity sensors are included in the following sections.

5.2. Transmissive and Reflective Measurements with Remote and Proximity MSW Sensors

5.2.1. Transmissive Measurements

For transmissive measurements using photonic, radiowave, or X-ray techniques, the electromagnetic (EM) wave incident on the waste surface interact with matter with a decaying intensity over the waste sample depth. The EM wave absorption in materials can be described by (4) or (5a). Transmissive measurements for photonic and radiowave sensors highly depend on absorption or scattering, whereas for X-ray techniques, transmissive intensity highly depend on the absorption and Compton scattering. For inductance sensors (assuming the excitation and pick-up coil are on opposite sides of the waste volume for transmissive measurement), the signal intensity from the eddy currents induced by the magnetic flux incident on waste surface is dependent on the conductivity of the waste sample. As seen in (12), the skin depth is inversely proportional to the square root of conductivity and angular frequency of the charges in motion. The signal intensity of the transmissive measurements with inductance sensors depend on the metal content and the bulk-size of waste materials. For capacitance sensors (assuming electrodes are on opposite sides of the waste volume for transmissive measurement), the dielectric measurements of waste materials for metal or moisture detection are highly dependent on waste bulk-size and electrode distance, as seen in (7).

5.2.2. Reflective Measurements

The signal intensity from EM waves reflecting off a waste surface depend on the energy exchange events with molecules, as well as the scattering events of the EM wave at the surface or within the interaction depth of a material. The reflected signal intensity at the interface of two materials is dependent on their complex refractive index seen from (3). Reflective measurements for photonic and radiowave sensors depend on the scattering events of materials as well as the complex refractive index. Reflective measurements for X-ray techniques depend on the photoabsorption in materials inducing photon emission or Compton scattering events that induce inelastic scattered photons. For inductance sensors in reflective settings (excitation and pick-up coil are on the same side of the waste volume), the intensity is a function of the depth-position of conductive materials in waste that also depends on the skin depth of the magnetic flux incident on the bulk waste sample. For capacitance sensors (with both electrodes on the same side of the waste volume) in reflective settings, the capacitance measurements can be related to moisture content in waste.

5.2.3. Assessment of Sensor Techniques in Transmissive or Reflective Settings

The feasibility of using electric or magnetic sensors for monitoring fuel quality of waste based on moisture and metal content in the waste materials can be discussed in view of the sensor technique intensity dependence in reflective and transmissive settings. Capacitance sensors have low specificity in differentiating between metal or moisture detection since the parameters measured are based on detecting the dielectric change in materials. Increase in metal content and moisture will both result in an increase in the dielectric parameter. The capacitor will also short-circuit for high metal contents. In transmissive settings, it can be challenging to detect the dielectric change in materials independently of the volume of the waste samples. To reduce the cross-sensitivity for size changes in waste materials, shredding and conveyor belts can be used to obtain constant waste sample depth. Concerning inductance sensors, they have high specificity in detecting metal in waste due to detection of eddy currents from conductive materials. Depending on the conductivity of bulk waste materials, inductance sensors also obtain sufficient reflective and transmissive

intensities since different frequencies for magnetic flux generation can be used to optimize the trade-off between signal strength and skin depth, as seen in (11) and (12).

For X-ray techniques, the feasibility for fuel quality monitoring in waste can be discussed considering the use of soft and hard X-rays. The high rate of photoabsorption of soft X-ray in materials results in high attenuation and short penetration depths. Due to the high attenuation, this domain is not suitable for transmissive measurements. For reflective measurements, soft X-ray can be used for photoemission detection. The difference between incident photoabsorption and emitted X-ray wavelengths used in techniques such as X-ray fluorescence, spectroscopy, or imaging can be measured for characterizing elemental compositions in waste materials. In reflection and proximity settings, soft X-ray sensors are feasible for monitoring elemental compositions in waste. For hard X-ray, the high-energy domain and its interaction with matter are dominated by Compton scattering. Thus, hard X-rays will have high transmission intensities for materials with a large fraction of elements of low atom numbers and low transmission intensity for materials with a large fraction of elements of high atom numbers. Since most MSW compositions have a large fraction of elements with low atom numbers, hard X-rays may have a signal intensity that is possible to detect in transmissive settings. The intensity contrast between high and low atomic numbers visible in transmissive settings will also be visible in reflection settings. Therefore, in proximity settings, the hard X-ray sensor can be considered feasible in use for detecting different metals in both reflective or transmissive settings.

Radiowave and THz techniques can be discussed in view of the transmittance and reflectance dependence on moisture content in waste materials to assess the feasibility for monitoring the fuel quality. Using the assumptions described in Section 4.3, a computation is made of the transmittance in the frequency range 0.2–4.2 GHz for a 0.4 m waste thickness with varying water content, as shown in Figure 3.

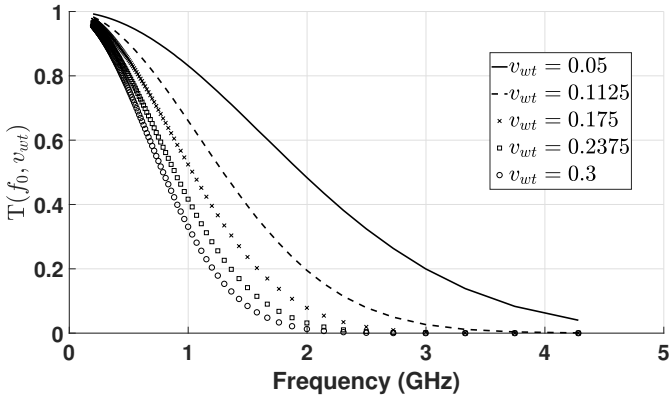

Figure 3. Transmittance as a function of frequency between 0.2–4.2 GHz with $d = 0.4$ m and v_{wt} between 0.05 and 0.3.

At $v_{wt} = 0.05$ and $v_{wt} = 0.3$, the transmittance is reduced to its half at 1.90 GHz and 0.78 GHz, respectively, illustrating the radiowave sensitivity to moisture. The change in transmittance as a function of distance between 0.2 and 1 m can also be computed with a constant water volume fraction at 0.3, as shown in Figure 4.

At 1.13 GHz and 0.3 GHz, a change in depth from 0.2 to 1 m reduces the transmittance from 0.5 to 0.02 and from 0.93 to 0.687, respectively. For frequencies higher than 2 GHz, the transmittance is lower than 0.1. The large variations in radiowave transmittance for different distances shows that there is a high cross-sensitivity for moisture and waste sample depth. With waste that has large variations in size or density, it can be challenging to relate the change in transmittance amplitude to the change in moisture.

Using the same parameters as used for the computation in Figure 3, but with frequencies in both the radiowave and THz domains, the reflectance is illustrated in Figures 5 and 6.

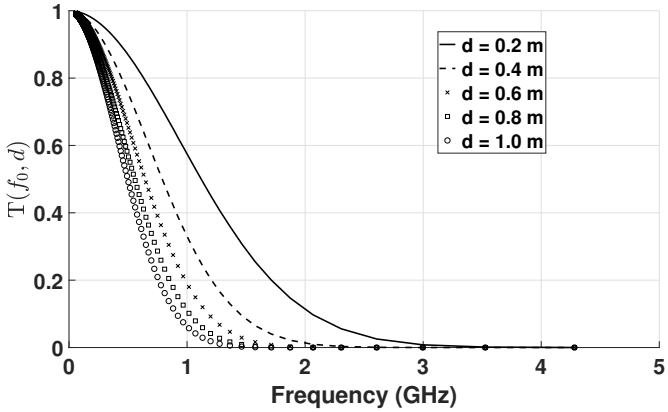

Figure 4. Transmittance as a function of frequency between 0.2–4.2 GHz with $v_{wt} = 0.3$ and d between 0.2 and 1 m.

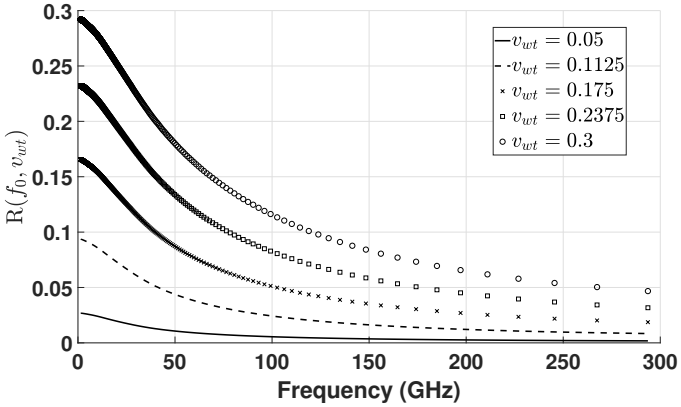

Figure 5. Radiowave reflectance as a function of frequency between 0.2–300 GHz and v_{wt} between 0.05 and 0.3.

From Figure 5, the change in reflectance as a function of increasing v_{wt} is larger for low frequencies than for high frequencies. In the THz domain, as seen in Figure 6, the reflectance is smaller than 0.05 for frequencies between 300–20,000 GHz. When comparing Figures 5 and 6, the change in reflectance as a function of v_{wt} is also significantly smaller in the THz domain than for the radiowave domain. The scattering effects of THz waves in waste materials would decrease the specificity of the reflectance amplitude change to moisture. Hence, even with an ideal material composition for the THz domain, it indicates that moisture detection with EM wave reflective measurements using frequencies in the radiowave domain is more feasible than using frequencies in the THz domain. The estimations presented above indicate that radiowave sensors have potential to be used as a remote sensor in reflective settings, while for radiowave sensors in transmissive settings and for THz sensors in reflective settings it is less feasible.

Considering UV–LWIR photonic techniques, their use in estimating fuel quality in waste materials can be assessed concerning the wavelength dependence of light–matter interactions. Single-point spectroscopy techniques can be conducted for the UV–LWIR domain, whereas multi- or hyperspectral imaging can be performed for the UV–SWIR domain. The penetration depth of light in the UV–LWIR domain is significantly short (orders of cm to mm) and unsuitable for transmissive measurements [122–124]. Reflection of UV–LWIR in materials can provide multiple and unique spectral fingerprints used for detecting specific material components. In the NIR–LWIR, these spectral fingerprints are more specific than in the UV–VIS; therefore, the detection of specific waste material can be feasible using single-point absorption spectroscopy or laser-induced breakdown spectroscopy (LIBS) in reflective settings.

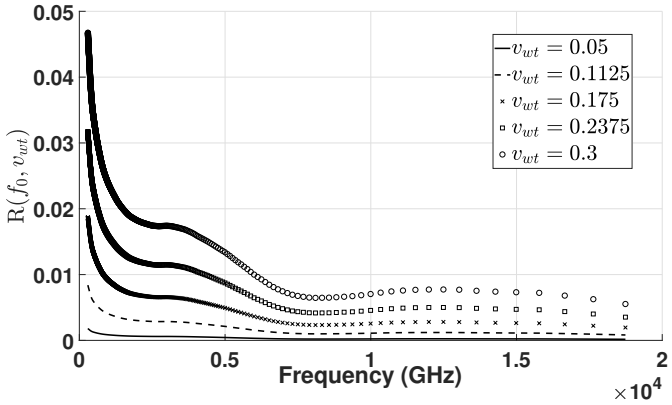

Figure 6. THz reflectance as a function of frequency between 300 GHz to 20 THz and v_{wt} between 0.05 and 0.3.

Multi- or hyperspectral imaging provides spectral and spatial parameters for sensing and can be adapted for detecting materials with a large variety in size, shape, or specific chemical entities in mixed compositions. The spectral–spatial features in images obtained with multi- or hyperspectral imaging techniques have been used for classification, linear, or nonlinear analysis by using supervised of unsupervised methods to identify or quantify specific components in mixed waste materials. Hence, due to the multiple sensor parameters available, the use of spectral imaging in the UV–LWIR wavelength shows great potential to be used as a remote sensor in reflective settings to identify or quantify specific waste materials related to fuel quality.

5.3. Feasibility of Using MSW Indicators for Assisting Waste-to-Energy Plant

5.3.1. Single-Point Spectroscopic Measurements

For single point spectroscopic measurements it can be challenging to deconvolve spectral intensity features that correspond to multiple specific materials in waste compositions. This challenge can result in low specificity. For X-ray spectroscopy measurements, the intensity dependence on elements with high or low atomic numbers will result in a high specificity for materials with density differences in waste compositions. Radiowave sensors have high specificity for both metal and moisture, but cannot differentiate between the intensity differences corresponding to either moisture or metal. The signal amplitude itself can also be challenging to relate to specific material components due to signal source instability, noise limitations of the signal detector, or drifting of the signal amplitudes. Challenges with specificity and sensitivity in single-point reflection or transmission spectroscopy measurements may limit the sensors only to be used for providing fuel quality values as indicators for alarms depending on the analytic methods used. However, the use of chemometric methods may provide solutions to improve specificity and sensitivity in detecting chemical components and materials.

5.3.2. Imaging Measurements

Concerning imaging measurements with X-ray or photonic techniques, the physical information obtained from the spatial dimensions can be used for estimating the volume ratio of detected materials. For large surface areas, the area of a specific material detected can be related to the volume using statistical analysis. For waste monitoring applications, studies have been conducted where components in waste derived fuels are classified in RGB images using an 11 × 11 dot grid to estimate the area of each waste fraction material [24–26]. The measured area was used with the bulk density of each waste component to estimate weight fraction. The use of an 11 × 11 dot grid to estimate the weight fraction of different waste components had a strong correlation with the original weight fraction values and showed that specific materials detected using surface monitoring represent the volume content of specific materials in a waste sample. Thus, the use of X-ray or photonic imaging

shows potential to be used for weight or volume fraction measurements of specific materials. This quantitative approach using imaging techniques to estimate fractions of specific materials have potential to be used for providing fuel parameters for process control.

6. Conclusions

This paper has critically assessed available sensor concepts, and their operating principles, for estimating fuel quality in MSW plants prior to incineration. Each group of sensors such as photonic, radiowave, electric or magnetic, or high-energy photon or particle sensors have been used for detecting a great variety of waste entities for waste sorting applications. The feasibility assessment here, on the other hand, was conducted concerning the sensor techniques to be installed and used in an operating WtE plant. The assessment concludes that remote and proximity sensors, applied in either transmissive or reflective settings, are preferred. For transmissive settings, it is most feasible to operate inductance and hard X-ray sensors, whereas for reflective settings, it is most feasible to operate photonic, low-frequency radiowave, soft and hard X-ray, and inductance sensors. The fuel quality estimation capacity for single-point measurements with photonic, radiowave, inductance, or X-ray techniques is limited to provide indicators for process alarms, while imaging measurements with photonic or X-ray techniques have the potential to provide parameters for both process control and indicators for alarms. The results present a first step in understanding which sensor solutions can be implemented for process control or alarm indicators. This knowledge and understanding will be important for guiding the evolution of the WtE industry in using new monitoring methods to measure fuel quality in waste, which will improve energy production stability, reduce the rate of incidental stops of waste incineration, and reduce risk of critical events.

In future work, remote monitoring techniques such as radiowave and photonic systems are recommended to be pursued and assessed for estimating the fuel quality in waste. Experiments and theoretical modeling should be conducted concerning moisture measurements in MSW with radiowave techniques in the low-frequency domain in reflective settings. Further investigation into using spectral imaging and deep learning for WtE processes is recommended to unveil the links between imaging parameters and fuel quality in waste so that objects and waste classes can be identified. The starting point for developing such a system can be built on earlier work, such as [14].

Author Contributions: H.I.D.I.M. and D.R.H. conceptualized the feasibility studies and prepared the original draft preparation. All authors have read and agreed to the published version of the manuscript.

Funding: This work was supported by the WtE 2030 funding (grant number: 280949) from the research council of Norway.

Data Availability Statement: Not applicable.

Acknowledgments: We want to acknowledge the valuable insight into waste-to-energy processes in Norway and the important feedback received on the applicability of selected sensor systems provided by SINTEF Energy (Trondheim), Returkraft (Kristiansand), and Statkraft Varme (Trondheim).

Conflicts of Interest: The authors declare no conflict of interest. The funders had no role in the design of the study; in the writing of the manuscript, or in the decision to publish the results.

References

1. Lee, U.; Han, J.; Wang, M. Evaluation of landfill gas emissions from municipal solid waste landfills for the life-cycle analysis of waste-to-energy pathways. *J. Clean. Prod.* **2017**, *166*, 335–342. [CrossRef]
2. Cucchiella, F.; D'Adamo, I.; Gastaldi, M. Sustainable waste management: Waste to energy plant as an alternative to landfill. *Energy Convers. Manag.* **2017**, *131*, 18–31. [CrossRef]
3. Aracil, C.; Haro, P.; Fuentes-Cano, D.; Gómez-Barea, A. Implementation of waste-to-energy options in landfill-dominated countries: Economic evaluation and GHG impact. *Waste Manag.* **2018**, *76*, 443–456. [CrossRef] [PubMed]
4. Gundupalli, S.P.; Hait, S.; Thakur, A. A review on automated sorting of source-separated municipal solid waste for recycling. *Waste Manag.* **2017**, *60*, 56–74. [CrossRef]

5. Cimpan, C.; Maul, A.; Jansen, M.; Pretz, T.; Wenzel, H. Central sorting and recovery of MSW recyclable materials: A review of technological state-of-the-art, cases, practice and implications for materials recycling. *J. Environ. Manag.* **2015**, *156*, 181–199. [CrossRef]
6. Vrancken, C.; Longhurst, P.J.; Wagland, S.T. Critical review of real-time methods for solid waste characterisation: Informing material recovery and fuel production. *Waste Manag.* **2017**, *61*, 40–57. [CrossRef]
7. Lombardi, L.; Carnevale, E.; Corti, A. A review of technologies and performances of thermal treatment systems for energy recovery from waste. *Waste Manag.* **2015**, *37*, 26–44; Special Thematic Issue: Waste-to-Energy Processes and Technologies. [CrossRef]
8. Hannan, M.; Abdulla Al Mamun, M.; Hussain, A.; Basri, H.; Begum, R. A review on technologies and their usage in solid waste monitoring and management systems: Issues and challenges. *Waste Manag.* **2015**, *43*, 509–523. [CrossRef]
9. Chromec, P.; Macher, S.S.; Kedrowski, C. WTE: Hitachi Zosen Inova Moving Grate and Anaerobic Digestion Technologies. In *Recovery of Materials and Energy from Urban Wastes*; Springer: Berlin/Heidelberg, Germany, 2019.
10. Ilani, T.; Herrmann, I.; Karnieli, A.; Arye, G. Characterization of the biosolids composting process by hyperspectral analysis. *Waste Manag.* **2016**, *48*, 106–114. [CrossRef]
11. Maestrojuan, I.; Martinez, A.; Crespo, G. THz water content analysis in biomass material. In Proceedings of the 2016 Global Symposium on Millimeter Waves (GSMM) & ESA Workshop on Millimetre-Wave Technology and Applications, Espoo, Finland, 6–8 June 2016; pp. 1–4.
12. Chandramohan, A.; Mendonca, J.; Shankar, N.R.; Baheti, N.U.; Krishnan, N.K.; Suma, M.S. Automated Waste Segregator. In Proceedings of the 2014 Texas Instruments India Educators Conference, TIIEC 2014, Bangalore, India, 4–5 April 2017. [CrossRef]
13. Mesina, M.B.; de Jong, T.P.; Dalmijn, W.L. Automatic sorting of scrap metals with a combined electromagnetic and dual energy X-ray transmission sensor. *Int. J. Miner. Process.* **2007**, *82*, 222–232. [CrossRef]
14. Muri, H.I.D.I.; Hjelme, D.R. Classification of municipal solid waste using deep convolutional neural network model applied to multispectral images. In *Automated Visual Inspection and Machine Vision IV*; Beyerer, J., Heizmann, M., Eds.; International Society for Optics and Photonics, SPIE: Bellingham, WA, USA, 2021; Volume 11787, pp. 97–108. [CrossRef]
15. Kumar, A.; Samadder, S.R. A review on technological options of waste to energy for effective management of municipal solid waste. *Waste Manag.* **2017**, *69*, 407–422. [CrossRef]
16. Abu-Qudais, M.; Abu-Qdais, H.A. Energy content of municipal solid waste in Jordan and its potential utilization. *Energy Convers. Manag.* **2000**, *41*, 983–991. [CrossRef]
17. Kathiravale, S.; Muhd Yunus, M.N.; Sopian, K.; Samsuddin, A.H.; Rahman, R.A. Modeling the heating value of Municipal Solid Waste. *Fuel* **2003**, *82*, 1119–1125. [CrossRef]
18. Komilis, D.; Kissas, K.; Symeonidis, A. Effect of organic matter and moisture on the calorific value of solid wastes: An update of the Tanner diagram. *Waste Manag.* **2014**, *34*, 249–255. [CrossRef]
19. Oller, S. Homogenization Theory. In *Numerical Simulation of Mechanical Behavior of Composite Materials*; Springer: Berlin/Heidelberg, Germany, 2014; pp. 113–153.
20. Yue, S.X.C.Z.X. Homogenization: In mathematics or physics? *arXiv* **2013**, arXiv:1302.0400.
21. Tanner, V.R. Die Entwicklung der Von-Roll-Müllverbrennungsanlagen (The development of the Von-Roll incinerators). *Schweiz. Bauztg.* **1965**, *83*, 251–260.
22. Götze, R.; Pivnenko, K.; Boldrin, A.; Scheutz, C.; Astrup, T.F. Physico-chemical characterisation of material fractions in residual and source-segregated household waste in Denmark. *Waste Manag.* **2016**, *54*, 13–26. [CrossRef]
23. Lausselet, C.; Cherubini, F.; del Alamo Serrano, G.; Becidan, M.; Strømman, A.H. Life-cycle assessment of a Waste-to-Energy plant in central Norway: Current situation and effects of changes in waste fraction composition. *Waste Manag.* **2016**, *58*, 191–201. [CrossRef]
24. Peddireddy, S.; Longhurst, P.J.; Wagland, S.T. Characterising the composition of waste-derived fuels using a novel image analysis tool. *Waste Manag.* **2015**, *40*, 9–13. [CrossRef]
25. Wagland, S.T.; Veltre, F.; Longhurst, P.J. Development of an image-based analysis method to determine the physical composition of a mixed waste material. *Waste Manag.* **2012**, *32*, 245–248. [CrossRef]
26. Wagland, S.T.; Dudley, R.; Naftaly, M.; Longhurst, P.J. Determination of renewable energy yield from mixed waste material from the use of novel image analysis methods. *Waste Manag.* **2013**, *33*, 2449–2456. [CrossRef] [PubMed]
27. Kimura, S.; Takagi, Y.; Tone, S.; Otake, T. A rate equation for gas-solid reactions accounting for the effect of solid structure and its application. *J. Chem. Eng. Jpn.* **1981**, *14*, 456–461. [CrossRef]
28. Hodoušek, M.; Böhm, M.; Součková, A.; Hýsek, Š. Effect of Moisture Content on the Air Permeability of Oriented Strand Boards. *BioResources* **2018**, *13*, 4856–4869.
29. Das, B.; Das, A.; Kothari, V.; Fanguiero, R.; Araujo, M.D. Moisture Flow through Blended Fabrics—Effect of Hydrophilicity. *J. Eng. Fibers Fabr.* **2009**, *4*, 155892500900400405. [CrossRef]
30. Amiot, M.; Lewandowski, M.; Leite, P.; Thomas, M.; Perwuelz, A. An evaluation of fiber orientation and organization in nonwoven fabrics by tensile, air permeability and compression measurements. *J. Mater. Sci.* **2014**, *49*, 52–61. [CrossRef]
31. Klinghoffer, N.B.; Themelis, N.J.; Castaldi, M.J. 1-Waste to energy (WTE): An introduction. In *Waste to Energy Conversion Technology*; Woodhead Publishing Series in Energy; Klinghoffer, N.B., Themelis, N.J., Castaldi, M.J., Eds.; Woodhead Publishing: Cambridge, UK, 2013; pp. 3–14. [CrossRef]

32. Council, N.R. *Waste Incineration and Public Health*; National Academies Press: Washington, DC, USA, 2000.
33. Potrykus, A.; Kling, M. *Study to Develop a Guidance Document on the Definition and Classification of Hazardous Waste*; Technical Report; European Commission: Brussels, Belgium, 2015.
34. Øie Kolden, H.; Magnanelli, E. *Disturbance Rejection in MSWC Plants*; Technical Report; SINTEF Energy: Trondheim, Norway, 2019.
35. Leskens, M.; van't Veen, P.; van Kessel, L.; Bosgra, O.; den Hof, P.V. Improved Economic Operation of MSWC Plants with a New Model Based PID Control Strategy. *IFAC Proc. Vol.* **2010**, *43*, 655–660. [CrossRef]
36. Magnanelli, E.; Tranås, O.L.; Carlsson, P.; Mosby, J.; Becidan, M. Dynamic modeling of municipal solid waste incineration. *Energy* **2020**, *209*, 118426. [CrossRef]
37. Saleh, B.E.A.; Teich, M.C. *Fundamentals of Photonics*, 2nd ed.; Wiley: New York, NY, USA, 2007.
38. Palleschi, V. Laser-induced breakdown spectroscopy: Principles of the technique and future trends. *ChemTexts* **2020**, *6*, 18. [CrossRef]
39. Gans, R. The Form of Ultramicroscopic Gold Particles. *Ann. Phys.* **1912**, *37*, 881–900. [CrossRef]
40. Mie, G. Beiträge zur Optik trüberber Medien, speziell kolloidaler Metallösungen. *Ann. Phys.* **1908**, *330*, 377–442. [CrossRef]
41. Muri, H.I.D.I. Novel Fiber Optic Biosensors Based on Nanoplasmonic and Interferometric Modalities. Ph.D. Thesis, Norwegian University of Science and Technology Faculty of Information Technology and Electrical Engineering Department of Electronic Systems, Torgarden, Norway, 2018. [CrossRef]
42. Huber, N.; Eschlböck-Fuchs, S.; Scherndl, H.; Freimund, A.; Heitz, J.; Pedarnig, J. In-line measurements of chlorine containing polymers in an industrial waste sorting plant by laser-induced breakdown spectroscopy. *Appl. Surf. Sci.* **2014**, *302*, 280–285. [CrossRef]
43. Masoumi, H.; Safavi, S.; Khani, Z. Identification and Classification of Plastic Resins using Near Infrared Reflectance. *World Acad. Sci. Eng. Technol.* **2012**, *6*, 877–884.
44. Kassouf, A.; Maalouly, J.; Rutledge, D.N.; Chebib, H.; Ducruet, V. Rapid discrimination of plastic packaging materials using MIR spectroscopy coupled with independent components analysis (ICA). *Waste Manag.* **2014**. [CrossRef]
45. Vassilev, V.; Stoew, B.; Blomgren, J.; Andersson, G. A mm-Wave Sensor for Remote Measurement of Moisture in Thin Paper Layers. *IEEE Trans. Terahertz Sci. Technol.* **2015**, *5*, 770–778. [CrossRef]
46. Serranti, S.; Gargiulo, A.; Bonifazi, G. Characterization of post-consumer polyolefin wastes by hyperspectral imaging for quality control in recycling processes. *Waste Manag.* **2011**, *31*, 2217–2227. [CrossRef]
47. Lee, Y.S. *Principles of Terahertz Science and Technology*; Springer Science & Business Media: New York, NY, USA, 2009; Volume 170.
48. Gundupalli, S.P.; Hait, S.; Thakur, A. Multi-material classification of dry recyclables from municipal solid waste based on thermal imaging. *Waste Manag.* **2017**, *70*, 13–21. [CrossRef]
49. Scott, D.M. A two-colour near-infrared sensor for sorting recycled plastic waste. *Meas. Sci. Technol.* **1995**, *6*, 156. [CrossRef]
50. Gurell, J.; Bengtson, A.; Falkenström, M.; Hansson, B.A. Laser induced breakdown spectroscopy for fast elemental analysis and sorting of metallic scrap pieces using certified reference materials. *Spectrochim. Acta-Part B At. Spectrosc.* **2012**, *74–75*, 46–50. [CrossRef]
51. Anzano, J.; Casanova, M.E.; Bermúdez, M.S.; Lasheras, R.J. Rapid characterization of plastics using laser-induced plasma spectroscopy (LIPS). *Polym. Test.* **2006**, *25*, 623–627. [CrossRef]
52. Larkin, P. *Infrared and Raman Spectroscopy: Principles and Spectral Interpretation*; Elsevier: Amsterdam, The Netherlands, 2017.
53. Charnier, C.; Latrille, E.; Jimenez, J.; Lemoine, M.; Boulet, J.C.; Miroux, J.; Steyer, J.P. Fast characterization of solid organic waste content with near infrared spectroscopy in anaerobic digestion. *Waste Manag.* **2017**, *59*, 140–148. [CrossRef]
54. Lesteur, M.; Latrille, E.; Maurel, V.B.; Roger, J.M.; Gonzalez, C.; Junqua, G.; Steyer, J.P. First step towards a fast analytical method for the determination of Biochemical Methane Potential of solid wastes by near infrared spectroscopy. *Bioresour. Technol.* **2011**, *102*, 2280–2288. [CrossRef] [PubMed]
55. Fitamo, T.; Triolo, J.M.; Boldrin, A.; Scheutz, C. Rapid biochemical methane potential prediction of urban organic waste with near-infrared reflectance spectroscopy. *Water Res.* **2017**, *119*, 242–251. [CrossRef] [PubMed]
56. Bonaccorsi, M.; Rateni, G.; Cavallo, F.; Dario, P. In-line industrial contaminants discrimination for the packaging sorting based on near-infrared reflectance spectroscopy: A proof of concept. In Proceedings of the IEEE Sensors, Glasgow, UK, 29 October–1 November 2017. [CrossRef]
57. Safavi, S.M.; Masoumi, H.; Mirian, S.S.; Tabrizchi, M. Sorting of polypropylene resins by color in MSW using visible reflectance spectroscopy. *Waste Manag.* **2010**, *30*, 2216–2222. [CrossRef] [PubMed]
58. Liu, D.; Sun, D.W.; Qu, J.; Zeng, X.A.; Pu, H.; Ma, J. Feasibility of using hyperspectral imaging to predict moisture content of porcine meat during salting process. *Food Chem.* **2014**, *152*, 197–204. [CrossRef]
59. Makantasis, K.; Karantzalos, K.; Doulamis, A.; Doulamis, N. Deep supervised learning for hyperspectral data classification through convolutional neural networks. In Proceedings of the 2015 IEEE International Geoscience and Remote Sensing Symposium (IGARSS), Milan, Italy, 26–31 July 2015; pp. 4959–4962. [CrossRef]
60. Gewali, U.B.; Monteiro, S.T.; Saber, E. Machine learning based hyperspectral image analysis: A survey. *arXiv* **2018**, arXiv:1802.08701.
61. Lapray, P.J.; Wang, X.; Thomas, J.B.; Gouton, P. Multispectral Filter Arrays: Recent Advances and Practical Implementation. *Sensors* **2014**, *14*, 21626–21659. [CrossRef]

62. ElMasry, G.; Sun, D.W. CHAPTER 1—Principles of Hyperspectral Imaging Technology. In *Hyperspectral Imaging for Food Quality Analysis and Control*; Sun, D.W., Ed.; Academic Press: San Diego, CA, USA, 2010; pp. 3–43. [CrossRef]
63. Koyanaka, S.; Kobayashi, K. Automatic sorting of lightweight metal scrap by sensing apparent density and three-dimensional shape. *Resour. Conserv. Recycl.* **2010**, *54*, 571–578. [CrossRef]
64. Huang, J.; Pretz, T.; Bian, Z. Intelligent solid waste processing using optical sensor based sorting technology. In Proceedings of the 2010 3rd International Congress on Image and Signal Processing, CISP 2010, Yantai, China, 16–18 October 2010. [CrossRef]
65. Bonifazi, G.; Serranti, S. Quality control by H yper S pectral I maging (HSI) in solid waste recycling: Logics, algorithms and procedures. In *Image Processing: Machine Vision Applications VII*; International Society for Optics and Photonics: Bellingham, WA, USA, 2014. [CrossRef]
66. Candiani, G.; Picone, N.; Pompilio, L.; Pepe, M.; Colledani, M. Characterization of fine metal particles derived from shredded WEEE using a hyperspectral image system: Preliminary results. *Sensors* **2017**, *17*, 1117. [CrossRef]
67. Van Den Broek, W.H.; Wienke, D.; Melssen, W.J.; Feldhoff, R.; Huth-Fehre, T.; Kantimm, T.; Buydens, L.M. Application of a spectroscopic infrared focal plane array sensor for on-line identification of plastic waste. *Appl. Spectrosc.* **1997**. [CrossRef]
68. Van Den Broek, W.H.; Wienke, D.; Melssen, W.J.; Buydens, L.M. Plastic material identification with spectroscopic near infrared imaging and artificial neural networks. *Anal. Chim. Acta* **1998**. [CrossRef]
69. Tatzer, P.; Wolf, M.; Panner, T. Industrial application for inline material sorting using hyperspectral imaging in the NIR range. *Real-Time Imaging* **2005**. [CrossRef]
70. Oyama, Y.; Zhen, L.; Tanabe, T.; Kagaya, M. Sub-terahertz imaging of defects in building blocks. *NDT E Int.* **2009**, *42*, 28–33. [CrossRef]
71. Bensalem, M.; Sommier, A.; Mindeguia, J.C.; Batsale, J.C.; Pradere, C. Terahertz Measurement of the Water Content Distribution in Wood Materials. *J. Infrared Millim. Terahertz Waves* **2018**, *39*, 195–209. [CrossRef]
72. Tanabe, T.; Kanai, T.; Kuroo, K.; Nishiwaki, T.; Oyama, Y. Non-Contact Terahertz Inspection of Water Content in Concrete of Infrastructure Buildings. *World J. Eng. Technol.* **2018**, *6*, 6. [CrossRef]
73. Zhang, H.B.; Mitobe, K.; Yoshimura, N. Application of Terahertz Imaging to Water Content Measurement. *Jpn. J. Appl. Phys.* **2008**, *47*, 8065–8070. [CrossRef]
74. Dworak, V.; Augustin, S.; Gebbers, R. Application of Terahertz Radiation to Soil Measurements: Initial Results. *Sensors* **2011**, *11*, 9973–9988. [CrossRef]
75. Nie, P.; Qu, F.; Lin, L.; Dong, T.; He, Y.; Shao, Y.; Zhang, Y. Detection of Water Content in Rapeseed Leaves Using Terahertz Spectroscopy. *Sensors* **2017**, *17*, 2830. [CrossRef]
76. Banerjee, D.; von Spiegel, W.; Thomson, M.D.; Schabel, S.; Roskos, H.G. Diagnosing water content in paper by terahertz radiation. *Opt. Express* **2008**, *16*, 9060–9066. [CrossRef]
77. Jördens, C.; Wietzke, S.; Scheller, M.; Koch, M. Investigation of the water absorption in polyamide and wood plastic composite by terahertz time-domain spectroscopy. *Polym. Test.* **2010**, *29*, 209–215. [CrossRef]
78. Parasoglou, P.; Parrott, E.P.J.; Zeitler, J.A.; Rasburn, J.; Powell, H.; Gladden, L.F.; Johns, M.L. Quantitative moisture content detection in food wafers. In Proceedings of the 2009 34th International Conference on Infrared, Millimeter, and Terahertz Waves, Busan, Korea, 21–25 September 2009; pp. 1–2.
79. Zhan, H.; Wu, S.; Bao, R.; Zhao, K.; Xiao, L.; Ge, L.; Shi, H. Water adsorption dynamics in active carbon probed by terahertz spectroscopy. *RSC Adv.* **2015**, *5*, 14389–14392. [CrossRef]
80. Parker, M. Chapter 18—Radar Basics. In *Digital Signal Processing 101*, 2nd ed.; Parker, M., Ed.; Newnes: Oxford, UK, 2017; pp. 231–240. [CrossRef]
81. Bishop, O. 24—Microwaves. In *Understand Electronics*, 2nd ed.; Bishop, O., Ed.; Newnes: Oxford, UK, 2001; pp. 283–296. [CrossRef]
82. Frenzel, L.E. Chapter 7—Radio/Wireless: The Invisible Cables of Modern Electronics. In *Electronics Explained*, 2nd ed.; Frenzel, L.E., Ed.; Newnes: Oxford, UK, 2018; pp. 159–194. [CrossRef]
83. Stuchly, M.A. *Fundamentals of the Interactions of Radio Frequency and Microwave Energies with Matter BT—Biological Effects and Dosimetry of Nonionizing Radiation: Radiofrequency and Microwave Energies*; Springer: Boston, MA, USA, 1983; pp. 75–93.
84. Nelson, S.O.; Trabelsi, S. Principles for Microwave Moisture and Density Measurement in Grain and Seed. *J. Microw. Power Electromagn. Energy* **2004**, *39*, 107–117. [CrossRef]
85. La Gioia, A.; Porter, E.; Merunka, I.; Shahzad, A.; Salahuddin, S.; Jones, M.; O'Halloran, M. Open-Ended Coaxial Probe Technique for Dielectric Measurement of Biological Tissues: Challenges and Common Practices. *Diagnostics* **2018**, *8*, 40. [CrossRef]
86. Trabelsi, S.; Nelson, S.O. Nondestructive sensing of physical properties of granular materials by microwave permittivity measurement. *IEEE Trans. Instrum. Meas.* **2006**, *55*, 953–963. [CrossRef]
87. Beneroso, D.; Albero-Ortiz, A.; Monzó-Cabrera, J.; Díaz-Morcillo, A.; Arenillas, A.; Menéndez, J.A. Dielectric characterization of biodegradable wastes during pyrolysis. *Fuel* **2016**, *172*, 146–152. [CrossRef]
88. Trabelsi, S.; Nelson, S.O. Microwave moisture meter for granular and particulate materials. In Proceedings of the 2010 IEEE International Instrumentation and Measurement Technology Conference, I2MTC 2010-Proceedings, Austin, TX, USA, 3–6 May 2010. [CrossRef]
89. McKeown, M.S.; Trabelsi, S.; Tollner, E.W. Effects of temperature and material on sensing moisture content of pelleted biomass through dielectric properties. *Biosyst. Eng.* **2016**. [CrossRef]

90. Zajíček, R.; Oppl, L.; Vrba, J. Broadband measurement of complex permitivity using reflection method and coaxial probes. *Radioengineering* **2008**, *17*, 14–19.
91. Ferhat, M.; Vourc'h, E.; Daout, F.; Bore, T.; Delepine-Lesoille, S.; Gatabin, C. Broadband dielectric spectroscopy open ended probe for the characterization of dispersive materials. In Proceedings of the 11th International Conference on Electromagnetic Wave Interaction with Water and Moist Substance, Firenze, Italy, 23–27 May 2016.
92. Paz, A.M.; Trabelsi, S.; Nelson, S.O.; Thorin, E. Measurement of the Dielectric Properties of Sawdust Between 0.5 and 15 GHz. *IEEE Trans. Instrum. Meas.* **2011**, *60*, 3384–3390. [CrossRef]
93. Fraden, J. *Physical Principles of Sensing BT—Handbook of Modern Sensors: Physics, Designs, and Applications*; Springer International Publishing: Cham, Switzerland, 2016; pp. 69–154.
94. Fuchs, A.; Zangl, H.; Holler, G.; Brasseur, G. Design and analysis of a capacitive moisture sensor for municipal solid waste. *Meas. Sci. Technol.* **2008**. [CrossRef]
95. Brunet, P.; Clément, R.; Bouvier, C. Monitoring soil water content and deficit using Electrical Resistivity Tomography (ERT)—A case study in the Cevennes area, France. *J. Hydrol.* **2010**. [CrossRef]
96. Gawande, N.A.; Reinhart, D.R.; Thomas, P.A.; McCreanor, P.T.; Townsend, T.G. Municipal solid waste in situ moisture content measurement using an electrical resistance sensor. *Waste Manag.* **2003**, *23*, 667–674. [CrossRef]
97. Kirkham, M.B. *Chapter 8—Time Domain Reflectometry*; Academic Press: Boston, MA, USA, 2014; pp. 103–122. [CrossRef]
98. Cataldo, A.; De Benedetto, E.; Huebner, C.; Trebbels, D. TDR application for moisture content estimation in agri-food materials. *IEEE Instrum. Meas. Mag.* **2017**, *20*, 26–31. [CrossRef]
99. Bhuyan, H.; Scheuermann, A.; Bodin, D.; Becker, R. Use of Time Domain Reflectometry to Estimate Moisture and Density of Unbound Road Materials: Laboratory Calibration and Field Investigation. *Transp. Res. Rec. J. Transp. Res. Board* **2017**, *2655*, 71–81. [CrossRef]
100. Nagel, J.R. Induced Eddy Currents in Simple Conductive Geometries: Mathematical Formalism Describes the Excitation of Electrical Eddy Currents in a Time-Varying Magnetic Field. *IEEE Antennas Propag. Mag.* **2018**, *60*, 81–88. [CrossRef]
101. O'Toole, M.D.; Karimian, N.; Peyton, A.J. Classification of nonferrous metals using magnetic induction spectroscopy. *IEEE Trans. Ind. Inform.* **2018**, *14*, 3477–3485. [CrossRef]
102. Oladapo, B.I.; Balogun, V.A.; Adeoye, A.O.; Ijagbemi, C.O.; Oluwole, A.S.; Daniyan, I.A.; Esoso Aghor, A.; Simeon, A.P. Model design and simulation of automatic sorting machine using proximity sensor. *Eng. Sci. Technol. Int. J.* **2016**, *19*, 1452–1456. [CrossRef]
103. Abdur Rahman, M.; Bakker, M.C. Hybrid sensor for metal grade measurement of a falling stream of solid waste particles. *Waste Manag.* **2012**, *32*, 1316–1323. [CrossRef]
104. Mesina, M.B.; De Jong, T.P.R.; Dalmijn, W.L. Improvements in separation of non-ferrous scrap metals using an electromagnetic sensor. *Phys. Sep. Sci. Eng.* **2003**. [CrossRef]
105. Kutila, M.; Viitanen, J.; Vattulainen, A. Scrap metal sorting with colour vision and inductive sensor array. In Proceedings of the International Conference on Computational Intelligence for Modelling, Control and Automation, CIMCA 2005 and International Conference on Intelligent Agents, Web Technologies and Internet, Vienna, Austria, 28–30 November 2005.
106. Hohlfeld, K.; Andreo, P.; Mattsson, O.; Simoen, J.P. Interaction of High-Energy Photon Beams with Matter. *J. ICRU* **2001**, *1*, 15–30. [CrossRef]
107. Gazis, E. The Ionizing Radiation Interaction with Matter, the X-ray Computed Tomography Imaging, the Nuclear Medicine SPECT, PET and PET-CT Tomography Imaging. In *Medical Imaging-Principles and Applications*; IntechOpen: Rijeka, Croatia, 2019.
108. Berger, M.; Yang, Q.; Maier, A. X-ray Imaging. In *Medical Imaging Systems*; Springer: Berlin/Heidelberg, Germany, 2018; pp. 119–145.
109. Maser, J. Soft X-rays and Extreme Ultraviolet Radiation: Principles and Applications. David Attwood. 1999. Cambridge University Press, Cambridge, UK. 470 pages. (hardback, $59.95). *Microsc. Microanal.* **2001**, *7*, 536.
110. Attwood, D.; Sakdinawat, A. *X-rays and Extreme Ultraviolet Radiation: Principles and Applications*; Cambridge University Press: Cambridge, UK, 2017.
111. Potts, P.J. *X-ray Fluorescence Analysis: Principles and Practice of Wavelength Dispersive Spectrometry BT—A Handbook of Silicate Rock Analysis*; Springer: Dordrecht, The Netherlands, 1987; pp. 226–285.
112. Osipov, S.P.; Usachev, E.Y.; Chakhlov, S.V.; Shchetinkin, S.A.; Osipov, O.S. Specific Features of Material Recognition by the Multi-Energy X-ray Method. *Russ. J. Nondestruct. Test.* **2019**, *55*, 308–321. [CrossRef]
113. Knapp, H.; Neubert, K.; Schropp, C.; Wotruba, H. Viable Applications of Sensor-Based Sorting for the Processing of Mineral Resources. *ChemBioEng Rev.* **2014**, *1*, 86–95. [CrossRef]
114. Chanasyk, D.S.; Naeth, M.A. Field measurement of soil moisture using neutron probes. *Can. J. Soil Sci.* **1996**, *76*, 317–323. [CrossRef]
115. Fayer, M.J.; Gee, G.W. *Neutron Scattering*; Elsevier: Oxford, UK, 2005; pp. 6–12. [CrossRef]
116. Gardner, W.H. *Water Content*; American Society of Agronomy-Soil Science Society of America: Madison, WI, USA, 2018. [CrossRef]
117. Yuen, S.T.S.; McMahon, T.A.; Styles, J.R. Monitoring in situ moisture content of municipal solid waste landfills. *J. Environ. Eng.* **2000**, *126*, 1088–1095. [CrossRef]

118. Bonifazi, G.; Serranti, S.; Rem, P.C. Hydrogen content and calorific value of municipal solid waste: Innovative quality control strategies of waste fed to incinerators. In *Waste Management and the Environment IV*; Zamorano, M., Ed.; WIT Press: Southampton, UK, 2008; pp. 289–298.
119. Becidan, M.; Wang, L.; Fossum, M.; Midtbust, H.O.; Stuen, J.; Bakken, J.I.; Evensen, E. Norwegian waste-to-energy (WtE) in 2030: Challenges and opportunities. *Chem. Eng. Trans.* **2015**, *43*, 2401–2406.
120. Chýlek, P.; Srivastava, V.; Pinnick, R.G.; Wang, R.T. Scattering of electromagnetic waves by composite spherical particles: Experiment and effective medium approximations. *Appl. Opt.* **1988**, *27*, 2396–2404. [CrossRef]
121. Segelstein, D.J. The Complex Refractive Index of Water. Ph.D. Dissertation, University of Missouri, Kansas City, MO, USA, 1981.
122. Lammertyn, J.; Peirs, A.; De Baerdemaeker, J.; Nicolaıi, B. Light penetration properties of NIR radiation in fruit with respect to non-destructive quality assessment. *Postharvest Biol. Technol.* **2000**, *18*, 121–132. [CrossRef]
123. Stolik, S.; Delgado, J.A.; Pérez, A.; Anasagasti, L. Measurement of the penetration depths of red and near infrared light in human ex vivo tissues. *J. Photochem. Photobiol. B Biol.* **2000**, *57*, 90–93. [CrossRef]
124. Lee, C.G. Calculation of light penetration depth in photobioreactors. *Biotechnol. Bioprocess Eng.* **1999**, *4*, 78–81. [CrossRef]